Supplemental Figures and Legends

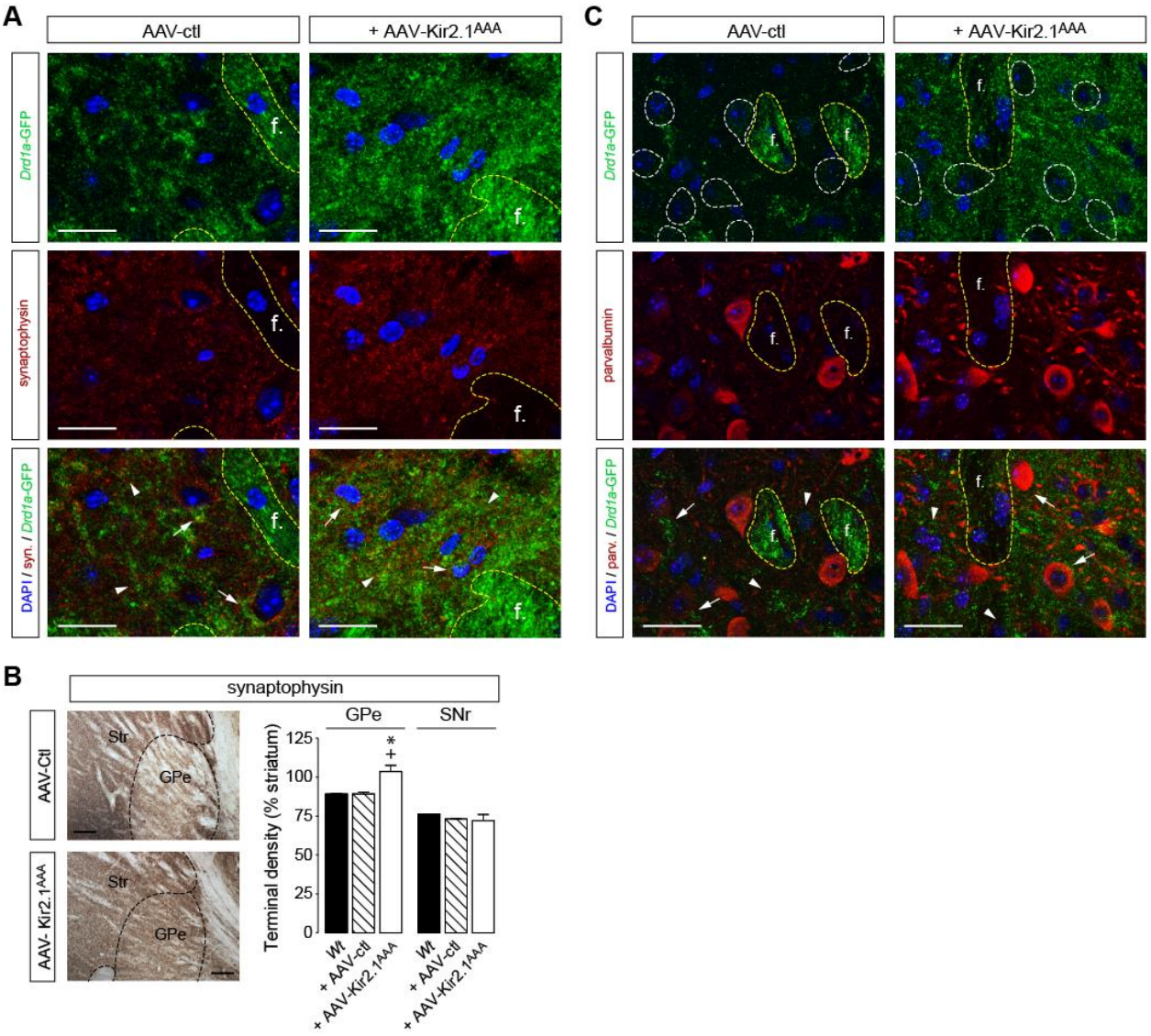

Figure S1. Bridging collaterals form presynaptic terminals that contact GPe cells and that are regulated by MSN excitability; Related to Figure 1.

(A) Coronal sections showing GFP-labeled striatonigral terminals co-localizing with the presynaptic vesicles marker synaptophysin in the GPe of mice injected with AAV-ctl or AAV-Kir2.1^{AAA}. GFP+synaptophysin-positive terminals contact GPe cell soma (arrows) and neuropil (arrowheads). This distribution is not changed when the density is increased in Kir2.1^{AAA}-injected mice. **(B)** Quantification of presynaptic terminals density in the GPe and

SNr of wild-type mice and AAV-ctl- or AAV-Kir2.1^{AAA}-injected mice using synaptophysin immunostaining. Left panel shows examples of synaptophysin immunostaining in AAV-ctl or AAV-Kir2.1^{AAA} mice. *p<0.05 compared to *Wt*; ^{+}p<0.05, compared to *Wt* + AAV-ctl; (n=4 mice/group). Scale bars, 200 µm. **(C)** Coronal sections showing GFP-labeled striatonigral terminals (green) and PV-positive cells (red) in the GPe of mice injected with AAV-ctl or AAV-Kir2.1^{AAA}. GFP-positive terminals contact both PV-positive (arrows) and PV-negative (arrowheads) cells. This distribution is not changed when the density is increased in Kir2.1^{AAA}-injected mice. f., passing fibers. Scale bars, 20 µm.

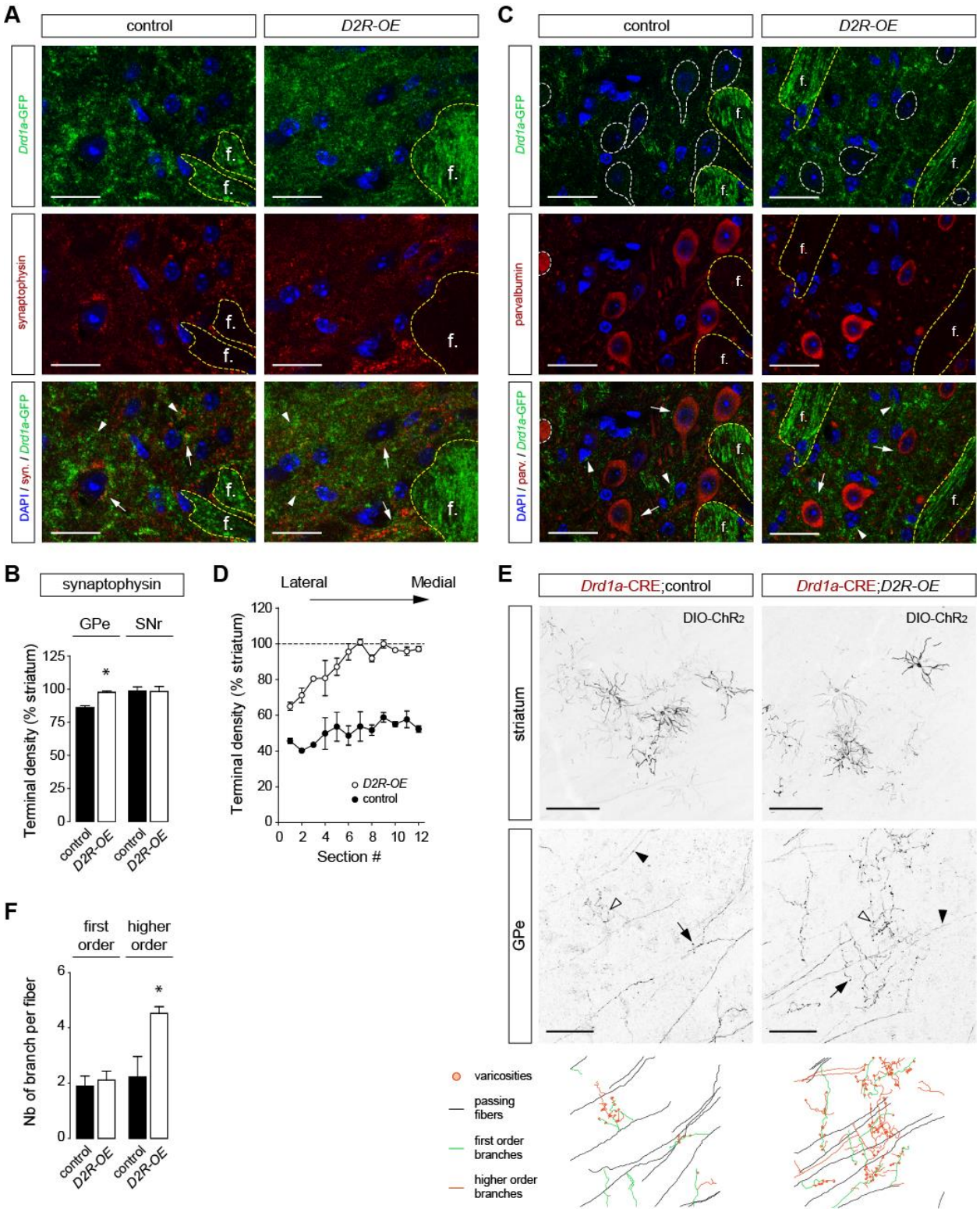
A
control
D2R-OE
Drd1a-GFP
synaptophysin
DAPI / syn. / Drd1a-GFP
f.
C
control
D2R-OE
Drd1a-GFP
parvalbumin
DAPI / parv. / Drd1a-GFP
f.
B
synaptophysin
GPe
SNr
Terminal density (% striatum)
125
100
75
50
25
0
*
control
D2R-OE
control
D2R-OE
D
Lateral
Medial
Terminal density (% striatum)
120
100
80
60
40
20
0
D2R-OE
control
0 2 4 6 8 10 12
Section #
E
Drd1a-CRE;control
Drd1a-CRE;D2R-OE
striatum
GPe
DIO-ChR2
DIO-ChR2
varicosities
passing fibers
first order branches
higher order branches
F
first order
higher order
Nb of branch per fiber
6
4
2
0
*
control
D2R-OE
control
D2R-OE

Figure S2. Striatal D2R regulates striatonigral presynaptic terminals in the GPe of the adult brain; Related to Figure 2.

(A) Coronal sections showing GFP-labeled striatonigral terminals co-localizing with synaptophysin in the GPe of control and *D2R-OE* mice. GFP+synaptophysin-positive terminals contact GPe cell soma (arrows) and neuropil (arrowheads). This distribution is not changed in *D2R-OE* mice. f., passing fibers. Scale bars, 20 μm. **(B)** Quantification of total presynaptic terminals density in the GPe and SNr of control and *D2R-OE* mice using synaptophysin immunostaining. *p<0.05 compared to control mice; (n=4 mice/group). **(C)** Coronal sections showing GFP-labeled striatonigral terminals and PV-positive cells in the GPe of control and *D2R-OE* mice. The distribution of GFP-positive terminals contacting both PV-positive (arrows) and PV-negative (arrowheads) cells is not changed in *D2R-OE* mice. **(D)** Lateral to medial distribution of striatonigral terminal density in the GPe of control and *D2R-OE* mice. (n=3 mice/group). **(E)** Sagittal sections showing sparse expression of ChR2-eYFP in *Drd1a*-MSNs in the striatum (top), and passing fibers and collaterals branches (first order and higher order branches) in the GPe (bottom) of control and *D2R-OE* mice. Black arrowheads show striatonigral passing fibers, white arrowheads show collateral branches, and arrows show varicosities. Scale bars, 200 μm (up) and 50 μm (down). Bottom panels show tracings of striatonigral passing fibers, first-order and higher-order collateral branches, and varicosities in control and *D2R-OE* mice. **(F)** Quantification of the number of first-order and higher-order collateral branches per passing fiber in control and *D2R-OE* mice. *p<0.05 compared to control; (n=4 mice/group).

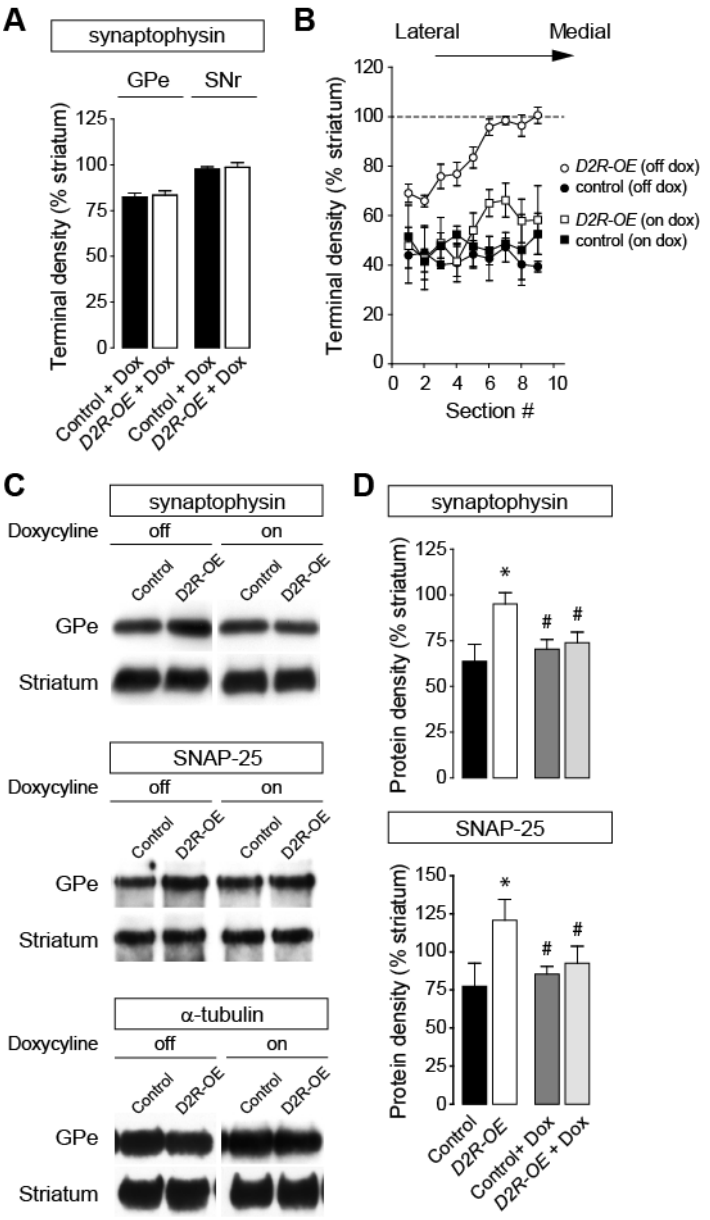

Figure S3. Increased presynaptic terminal density in the GPe of *D2R-OE* mice is reversed after restoring D2R expression to normal levels; Related to Figure 3.

(A) Quantification of total presynaptic terminals density using synaptophysin immunostaining in the GPe and SNr of control and *D2R-OE* mice treated with doxycycline for two weeks (*n*=4 mice/group). **(B)** Lateral to medial distribution of GPe striatonigral terminal density in control and *D2R-OE* mice treated or not with doxycycline for two weeks (*n*=3-4 mice/group). **(C)** Representative immunoblots showing density of α-tubulin and the presynaptic proteins synaptophysin and SNAP-25 in the GPe and striatum of control and

D2R-OE mice treated or not with doxycycline for two weeks. **(D)** Quantification of synaptophysin and SNAP-25 density in the GPe of control and *D2R-OE* mice treated or not with doxycycline for two weeks. *$p<0.05$, compared to control; $^{\#}p<0.05$, compared to *D2R-OE* (n=5-9 mice/group).

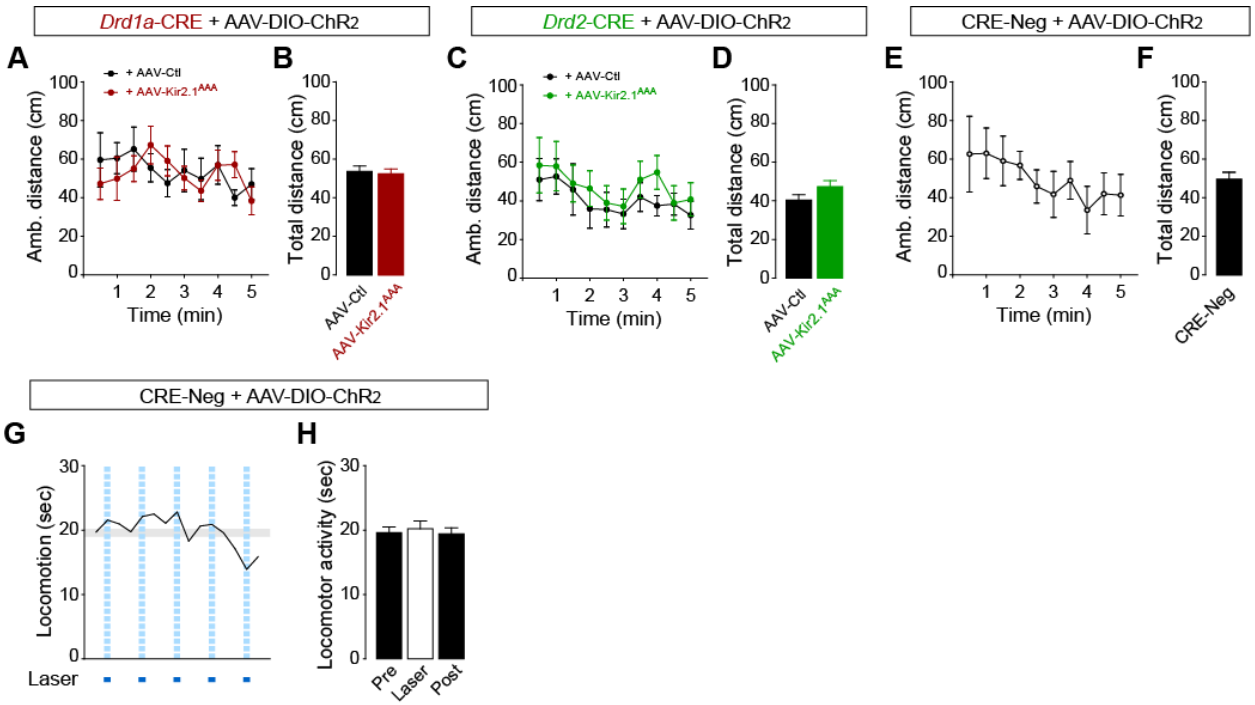

Figure S5. Striatal Kir2.1^{AAA} expression does not alter basal motor activity and CRE-negative mice do not respond to laser stimulation; Related to Figure 5.

(A-D) Basal (unstimulated) ambulatory activity during habituation is not affected by striatal expression of Kir2.1^{AAA} in *Drd1a*-CRE;DIO-ChR2 **(A,B)** or *Drd2*-CRE;DIO-ChR2 **(C,D)** mice. **(E,F)** Basal ambulatory activity of CRE-negative during habituation. **(G,H)** No effect of laser stimulation on locomotor activity of CRE-negative mice. **(G)** Trace showing locomotor activity during 5 consecutive pre-illumination/laser/post-illumination sessions in CRE-Negative;DIO-ChR2 mice. **(H)** Summary of motor activity measured in **(G)**. Data are mean only in **G**. Gray boxes represent s.e.m. of basal locomotion (pre+post); (*n*=5-6 mice/group).

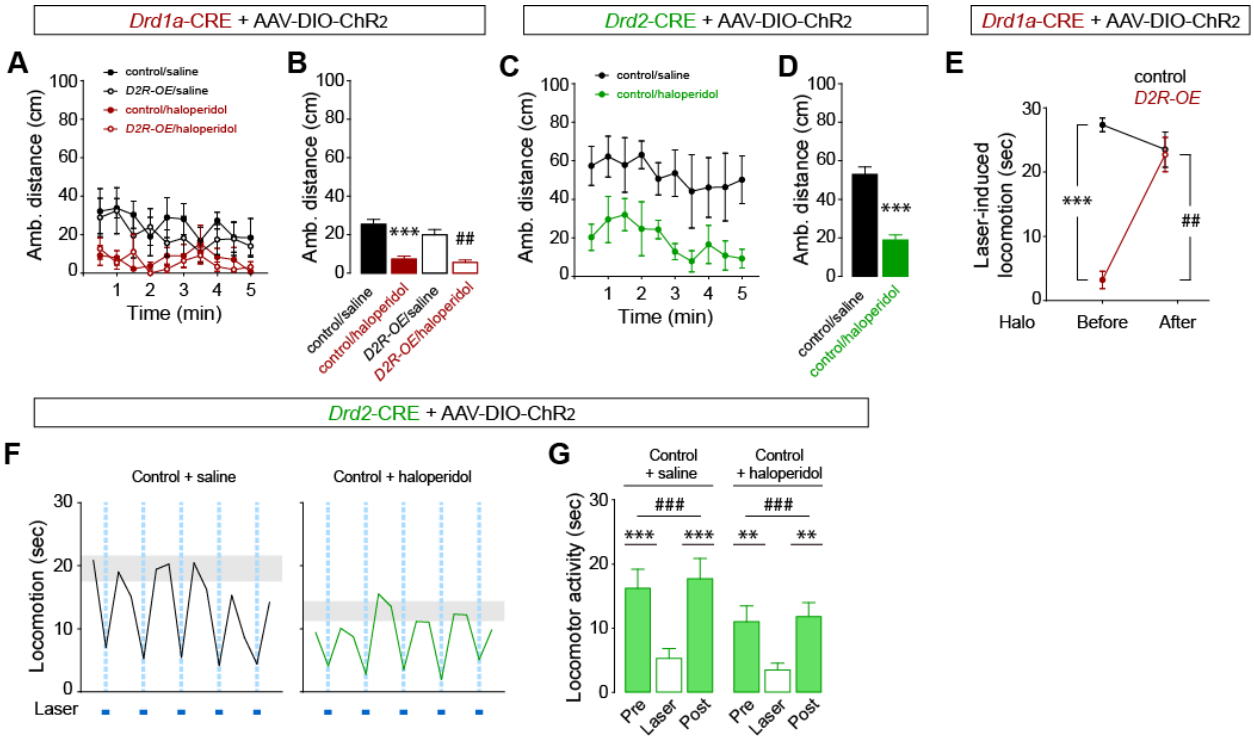

Figure S6. Chronic haloperidol treatment decreases basal ambulatory activity and rescues motor disruption in *D2R-OE* mice; Related to Figure 6.

(A-D) Basal (unstimulated) ambulatory activity during habituation is decreased in haloperidol-treated *Drd1a*-CRE;DIO-ChR2 **(A,B)** and *Drd2*-CRE;DIO-ChR2 **(C,D)** mice. **(B,D)** Summary of motor activity measured in **(A,C)**, respectively. ***p<0.001, compared to control/saline; $^{\#\#}p$<0.01, compared to *D2R-OE*/saline; (n=6-8 mice/group). **(E)** Within-subject longitudinal analysis showing laser-induced locomotor activity in control and *D2R-OE* mice before and after 2 weeks of haloperidol treatment. ***p<0.001, control *vs. D2R-OE* before treatment; $^{\#\#}p$<0.01, before *vs.* after in *D2R-OE* mice; (n=3 mice/group). **(F,G)** Optogenetic activation of the indirect pathway leads to similar motor inhibition in saline and haloperidol-treated mice. **(F)** Traces show locomotor activity in *Drd2*-CRE;DIO-ChR2 +saline or +chronic haloperidol mice. Gray boxes represent s.e.m. of basal locomotion (pre+post). **(G)** Summary of motor activity measured in **(F)**. $^{\#\#\#}p$<0.001, repeated *two-way* ANOVA. **p<0.01, ***p<0.001 compared to laser; (n=6 mice/group). Data are mean only in **F**. Gray boxes represent s.e.m. of basal locomotion (pre+post).

Supplemental Experimental Procedures

Behavioral analysis.

Motor activity was assessed in an open field box as described in (Kravitz et al., 2010) under ambient light conditions. Odor cues were eliminated by cleaning the box between animals. Two fiberoptic patch-cords were coupled via a zirconium sleeve (Doric Lenses) to the bilateral ferrules implanted into each mouse. Patch-cords were then connected to a 1:2 rotary joint optical commutator (Doric Lenses) via an FC adaptor to maintain steady light output and prevent patch-cord entanglement during locomotion. The patchcord/commutator combination was coupled to a solid-state 473nm 100mW laser. Light intensity was set to 2 mW illumination at the tip of each implanted fiber. Light stimulation was controlled using a Master-8 stimulator (AMP Instruments). After optical fibers were attached, mice were placed in the center of a plexiglas activity chamber (length, 45 cm; width, 45cm; height, 30 cm; model ENV-520, Med Associates) equipped with infrared detectors located 1.5 cm above the chamber floor and spaced 2.5 cm apart infrared detectors to track animal movement in the horizontal and vertical planes. After a 5-min habituation period without illumination, the laser was illuminated in a series of 5 sessions. Each session consisted in three consecutive 30-sec periods during which the laser was off ("Pre"), then on ("Laser", constant illumination), then off ("Post").

Total ambulatory distance was automatically scored using the Open Field Arena software (Med Associates). Mice were also video-monitored from above using a video camera and motor activity was scored upon three parameters: no activity (continuous periods of time during which the position of animal's center point did not change for at least 0.5 sec, excluding grooming), locomotor activity (continuous periods of time during which the animal initiated a movement, including vertical and horizontal activity), and resting (any movement that was none of the others, including grooming). These parameters were pre-determined after careful monitoring of the mice as follow: at least two mice of each group were video-taped in a home-made open field using a video camera placed horizontally at the level of the mice. All stereotypic and non-stereotypic behaviors under normal condition or that were triggered by laser illumination were carefully reported by at least two different observers and were cross-validated independently. Locomotion (defined as the

amount of time during which the mouse spent walking during a 30-second session) was then scored blind of the group condition and was averaged for each mouse over the 30-second bins for each condition (before, during and after laser illumination). In consequence the maximum time of locomotion cannot exceed 30 sec. Optical stimulation sites were reconstructed after each experiment. Mice were sacrificed and sagittal striatum sections were collected. Fiberoptic tracks were located in the slices and optical stimulation sites were determined by locating the site 0.5 mm ventral to the end of the fiberoptic tip.

In situ hybridization

Transgenic D2R expression was determined by *in situ* hybridization using a digoxigenin-labeled cRNA probe against the human growth hormone polyA sequence specific to the transgenic mRNA as described in (Kellendonk et al., 2006).

Immunoblotting.

Mice brains were quickly removed, washed in ice-cold PBS and snap-frozen in liquid nitrogen. 300-µm-thick frozen sections were obtained using a CM-3050-S cryostat (Leica) and striatal and pallidal tissues were extracted using Harris micropunches (Ted Pella, 1-mm diameter). Tissues from 5 mice were pooled as one sample and were homogenized in ice-cold 20 mM Tris-HCl, pH 7.4, 2 mM EDTA, 150 mM NaCl, 1% NP-40 with protease inhibitor cocktail (Complete, Roche) in a glass/Teflon-type mini-homogenizer. Lysates were centrifuged at 10,000 x *g* for 10 min at 4°C and the supernatant was collected. Equal amounts of proteins were subjected to 12% SDS-PAGE. Detection of α-tubulin (55 kDa), synaptophysin (37 kDa) and SNAP-25 (25 kDa) was performed on the same membrane using anti-α-tubulin (1:5,000; Sigma), anti-synaptophysin (1:1,000; Abcam), anti-SNAP-25 (1:5,000; Abcam) and appropriate HRP-conjugated secondary antibodies and autoradiography films, or fluorescence-conjugated secondary antibodies (680-nm and 780-nm) and an Odyssey infrared fluorescent scanner (LiCor). The experiment was repeated 3 times in duplicate. Proteins were quantified by densitometry using ImageJ (NIH).

Supplemental References

Kellendonk, C., Simpson, E.H., Polan, H.J., Malleret, G., Vronskaya, S., Winiger, V., Moore, H., and Kandel, E.R. (2006). Transient and selective overexpression of dopamine D2 receptors in the striatum causes persistent abnormalities in prefrontal cortex functioning.[see comment]. Neuron *49*, 603-615.

Kravitz, A.V., Freeze, B.S., Parker, P.R., Kay, K., Thwin, M.T., Deisseroth, K., and Kreitzer, A.C. (2010). Regulation of parkinsonian motor behaviours by optogenetic control of basal ganglia circuitry. Nature *466*, 622-626.